Electrochimica Acta 115 (2014) 189–196

Contents lists available at ScienceDirect

Electrochimica Acta

journal homepage: www.elsevier.com/locate/electacta

The effect of grid configurations on potential and current density distributions in positive plate of lead–acid battery via numerical modeling

Davood Nakhaie [a], Pooya Hosseini Benhangi [b,*], Akram Alfantazi [c], Ali Davoodi [d]

[a] Department of Materials Engineering, Faculty of Engineering, Ferdowsi University of Mashhad, PO Box 91775-1111, Mashhad, Iran
[b] Department of Chemical and Biological Engineering, The University of British Columbia, 2360 East Mall, Vancouver, BC V6T 1Z3, Canada
[c] Department of Materials Engineering, The University of British Columbia, 6350 Stores Road, Vancouver, BC V6T 1Z4, Canada
[d] Department of Materials and Polymers Engineering, Faculty of Engineering, Hakim Sabzevari University, Sabzevar, Iran

ARTICLE INFO

Article history:
Received 28 August 2013
Received in revised form 23 October 2013
Accepted 25 October 2013
Available online 1 November 2013

Keywords:
Grid configuration
Lead–acid battery
Numerical modeling

ABSTRACT

During the last decades, huge efforts have been made to enhance the efficiency as well as performance of lead–acid batteries. The configuration of grid wires plays an important role in minimizing the ohmic drop and hence, improving its current collecting ability. In the current study, numerical methods have been employed to investigate the effects of grid configuration on the performance of a positive electrode in lead–acid batteries. Potential and current density distributions have been modeled through grid wires, active material and adjacent electrolyte to the surface of each grid. The modeling results are consistent with experimental findings in the literature saying that the optimized diagonal design for grid configuration provides lower total grid weight as well as enhanced current collecting role comparing to other designs such as, conventional, diagonal and expanded metal. This confirms that numerical modeling is a fast, inexpensive and effective method for optimization of the battery grid configuration.

1. Introduction

During the last decade, huge efforts have been made to enhance efficiency and performance of lead–acid batteries, i.e. incorporating promising alloying elements including Ca, Sn, Ag, into the grid alloy, optimizing the grid configuration and applying additives to both active material and battery electrolyte [1–5].

Each grid of SLI (starting, lighting, and ignition) battery is usually made of two compartments; first, a rectangular frame surrounded a network of wires and second, a lug on top of the frame basically used for carrying the current in or out of the plate. During the discharge or charge process, electric current generated or applied moves through both lug and grid wires in opposite directions [6]. While the battery grid is mainly a precursor for the active material and absorbent for mechanical stress specially caused by external forces or volume changes of active mass during cycling, it is also responsible for current distribution through the plate [7].

In industrial scale, grids are usually manufactured via two different methods named as casting and expanded metal. While first method uses casted lead-alloy frame as a precursor for active material, expanded metal method employs a different idea. In this method, a strip of lead alloy sheet is subjected to pressure in guillotine fashion between slitting and stretching dies leading to a mesh-like plate with polygonal paste-retaining cells [7].

The configuration of grid wires plays an important role in minimizing the ohmic drop which could lead to uniform current distribution through the electrode. Such design could also introduce more reaction sites on the electrode [6,8].

Even though several attempts have been made to investigate the role of grid configuration on its potential and current density distributions, the effects of electrolyte and active material on these issues are not fully considered [6,9,10]. Numerical methods could help simulate the effects of such parameters on the battery performance instead of time consuming experimental studies [8]. In the present study, the potential and current density distributions have been modeled via numerical methods to study the effect of grid configuration on the performance of a positive electrode in lead–acid batteries. The effects of both electrolyte and active material have been also taken into account.

* Corresponding author. Tel.: +1 604 827 3198; fax: +1 604 822 6003.
E-mail address: phosseini@chbe.ubc.ca (P.H. Benhangi).

0013-4686/$ – see front matter.
http://dx.doi.org/10.1016/j.electacta.2013.10.152

2. Theory

The molar flux of a charged species (j) in an electrolyte arises from three transport mechanisms, i.e. migration, diffusion and convection.

$$N_j = -z_j \mu_j F C_j \nabla \Phi - D_j \nabla C_j + C_j \nu \quad (1)$$

where Nj is ionic flux, z_j charge, μ_j ionic electrochemical mobility, F is the Faraday's constant, C_j concentration, Φ electrostatic potential outside the electric double layer, D_j diffusion coefficient, ν bulk average fluid velocity, and ∇ differential operator, respectively. The total ionic current density (i) is given by assigning the charge to flux of each species and summing over all species:

$$i = F \sum_j z_j N_j \quad (2)$$

Substituting Eq. (2) into (1),

$$i = -F^2 \nabla \Phi \sum_j z_j^2 \mu_j C_j - F \sum_j z_j D_j \nabla C_j + F \nu \sum_j z_j C_j \quad (3)$$

The condition of electroneutrality in solution implies:

$$\sum_j z_j C_i = 0 \quad (4)$$

Therefore, the last term of Eq. (3) is zero. Considering no ionic concentration gradients in the electrolyte, Eq. (3) becomes ohm's law for ion transport in electrolytes:

$$i = \sigma \nabla \Phi \quad (5)$$

where σ is the specific electrolyte conductivity given by

$$\sigma = -F^2 \sum_j z_j^2 \mu_j C_j \quad (6)$$

In case when there is no homogenous reaction in the electrolyte involving the ionic species or its net effect is zero, we can say:

$$\tilde{N} i = 0 \quad (7)$$

From Eq. (5), one can say:

$$\nabla i = \sigma \nabla^2 \Phi \quad (8)$$

which results in the Laplace equation,

$$\nabla^2 \Phi = 0 \quad (9)$$

The overall overpotential at the electrode is also given by:

$$\eta = E - E_e - \Phi \quad (10)$$

where E is the electrode potential and E_e denotes the thermodynamic equilibrium potential.

In case of no ionic concentration gradient in the electrolyte of an electrochemical cell and perfectly reversible faradic reactions, the mass transport and kinetic limitations are negligible, respectively. In such condition, which the overpotential is associated with the ohmic drop, the Laplace equation can be solved by implementing following boundary conditions. At insulator boundary:

$$\nabla \Phi = 0 \quad (11)$$

and potential in the solution adjacent to the electrode is equal to the potential on the electronic conductor:

$$\Phi_0 + \Phi_m = \text{constant} \quad (12)$$

During charge and discharge process at positive electrodes of lead–acid batteries, the following electrochemical reaction takes place in forward and backward directions, respectively:

$$PbO_2 + 4H^+ + SO_4^{2-} + 2e^- \leftrightarrow PbSO_2 + 2H_2O \quad (13)$$

The equilibrium potential of the half-cell results in:

$$E_{e,PbO_2/PbSO_4} = 1.683 - 0.118\text{pH} + 0.029 \log a_{SO_4^{2-}} \quad (14)$$

An important parameter in designing battery plates is known to be

$$\alpha = W_g/(W_g + W_{am}) \quad (15)$$

where W_g is grid weight and W_{am} is the weight of active mass. The value of this ratio varies between 0.35 and 0.60. Since the plate capacity depends on its available active mass, the tendency is to minimize the value of α [7,11].

The conductivities of lead and lead oxide (PbO_2) are much higher than that of lead sulfate [12]. Hence, when PbO_2 converts to $PbSO_4$ during the discharge mode (cf. Eq. (13)), ohmic resistance of active material increases. Although employing additives, such as active carbon, titanium oxide and graphite, can improve conductivity of the active materials [11,13], it seems that some modifications in grid design could also solve the problem. For example, reduction in the mesh size of each grid could lead to more uniform potential and current density distribution through the grid [11]. It is worth mentioning that even though any decrease in mesh dimensions of a grid could lower its active mass consumption, smaller meshes would increase total grid weight hence the costs [11].

Since more currents are carried by wires near the lug in comparison to other parts of the grid, resistance characteristics of the grid can be improved by increasing the number of vertical wires as well as skewed ones. However, the former method could increase consumed lead and hence raise the grid weight. Therefore, the factor α increases which is not desirable [7]. Thus, a compromise has to be made between Pb consumption and grid design to lower plate resistivity without significant weight increase.

3. Model

Based on the theory explained in Section 2 and with the help of Comsol software, a 3D numerical model has been developed to investigate the potential and current density distribution of four different grid configurations. Fig. 1a shows the conventional grid configuration consisting of interconnected vertical and horizontal ribs surrounded by a rectangular frame with a lug located on the top right corner of the frame. Rectangular-like configuration of second grid, shown in Fig. 1b, consists of parallel horizontal ribs which are crossed by a series of skewed ribs headed toward the lug. Fig. 1c demonstrates configuration of the expanded metal grid. This grid comprises of a reticulated pattern of thin lead wires encompassed by a rectangular frame. It is worth mentioning that for the sake of better current collection, upper and lower edges of the frame are considered to be thicker than side edges in the latter configuration. It is assumed that dimensions of the frame, location and dimensions of the lug as well as thickness of the wires are similar in all cases. Table 1 shows specifications of three modeled grids, i.e. conventional, diagonal and expanded metal grids. In order to find the mass of each grid and its associated active material, their calculated volumes using modeling data has been multiplied by the densities of lead and lead oxide, respectively.

The existence of various materials in the different parts of the grids, i.e. grid alloy, active material and electrolyte, could severely

Table 1
Grid specifications as well as their design parameter.

Grid name	Grid weight (g)	Active mass weight (g)	Grid surface (cm^2)	α
Conventional	130.41	232.59	289.50	0.359
Diagonal	130.52	232.40	297.50	0.359
Expanded metal	130.29	232.68	256.60	0.358

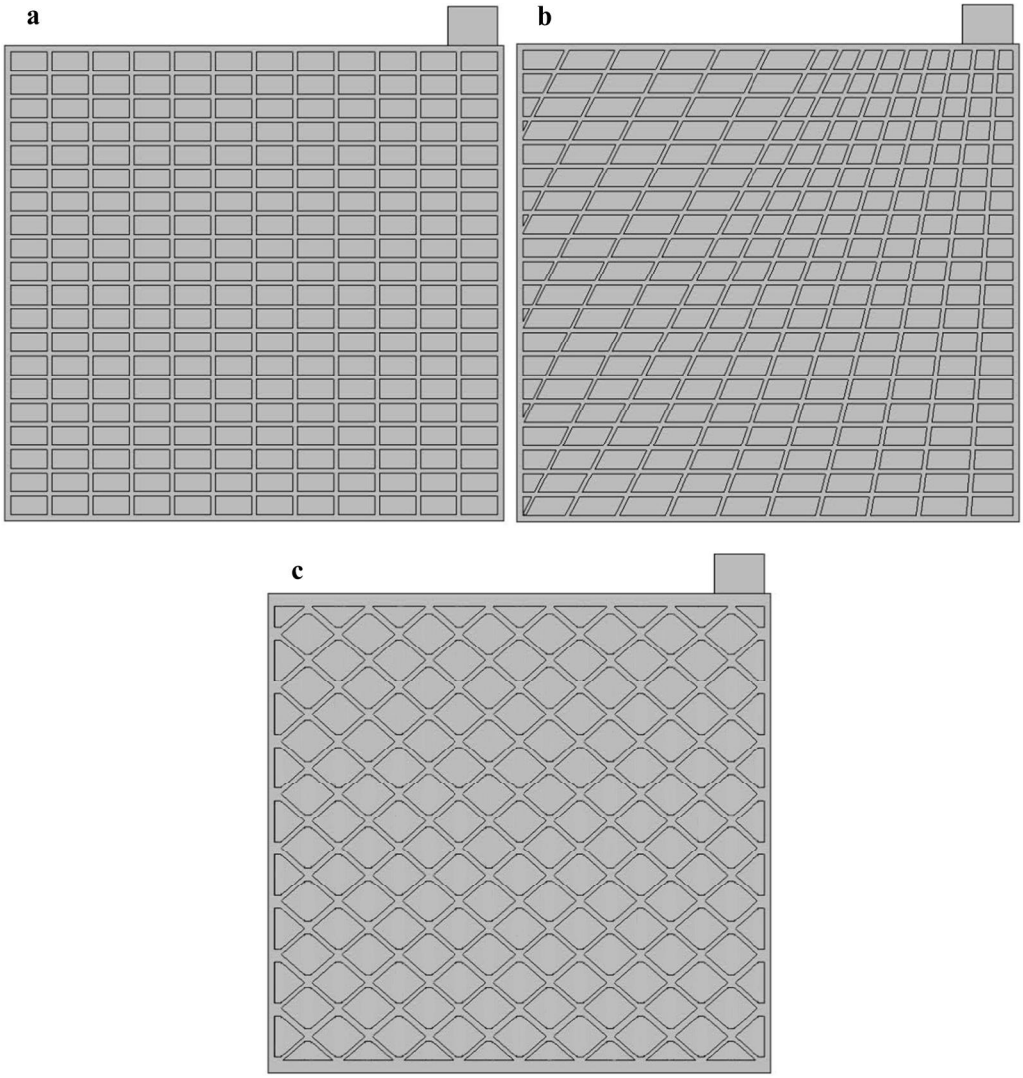

Fig. 1. A schematic of three different grid configurations applied to the model, i.e. (a) conventional grid, (b) diagonal grid, (c) expanded metal grid.

affect the potential and current distributions through each grid. This would lead to unfair comparison between studied cases. To eliminate this effect, same characteristics, e.g. conductivity, were employed for all of the materials in the applied model.

Fig. 2 shows a schematic of the domain as well as boundary conditions used to study the conventional grid. Triangular mesh was used with a maximum element size and element growth rate of 16.5 mm 1.5, respectively. It should be mentioned that the mesh size has been exaggerated for sake of better visual appearance in Fig. 2. The Laplace equation (*eq.* 9) governs the domain.

For a SLI lead–acid battery containing 4.8 M sulfuric acid as electrolyte, the equilibrium potential of its positive plate equals 1.761 V/SHE. This value was applied to the interface between electrolyte and electrode itself in the model. It is also assumed that no electron transfer takes place between the electronic conductor and species in the electrolyte. Hence, the difference between electrode potential and the potential in electrolyte adjacent to the electrode is equal to the same value at equilibrium, i.e.:

$$E = E_e \tag{16}$$

The grid boundaries were set as insulator where the current applied to the surface was zero.

According to Yamada et al., the current needed for an engine to start can be over 500 A [6]. Assuming that a cell consists of six positive plates, the current produced by each positive plate could be nearly 83.3 A. This current value was introduced to the lug of each grid in the model. The model was solved in stationary state.

4. Results and discussion

4.1. 4.1 Potential and current density distributions of conventional, diagonal and expanded metal grids

Fig. 3 shows the potential distribution in the described electrodes. It can be seen that the lug and its adjacent area possess lowest potential value in all cases. Moving away from this particular area, the potential gradually increases to its highest value for all three electrodes. This is also consistent with the experimental data from literature confirming that the lowest potential values is achieved for areas near the log in the positive battery plate during discharge [6,9,14]. Maximum and minimum potential values for each grid are tabulated in Table 2. Although maximum potential values for all cases are quiet similar, i.e. 1.730 V/SHE, its minimum values are slightly different from each other. It is observed that conventional grid shows highest potential difference of 95.7 mV while diagonal grid possesses the lowest one, i.e. 77.4 mV. Expanded metal grid ranks among these two grid configurations (Fig. 1a and b, Fig. 5a and b).

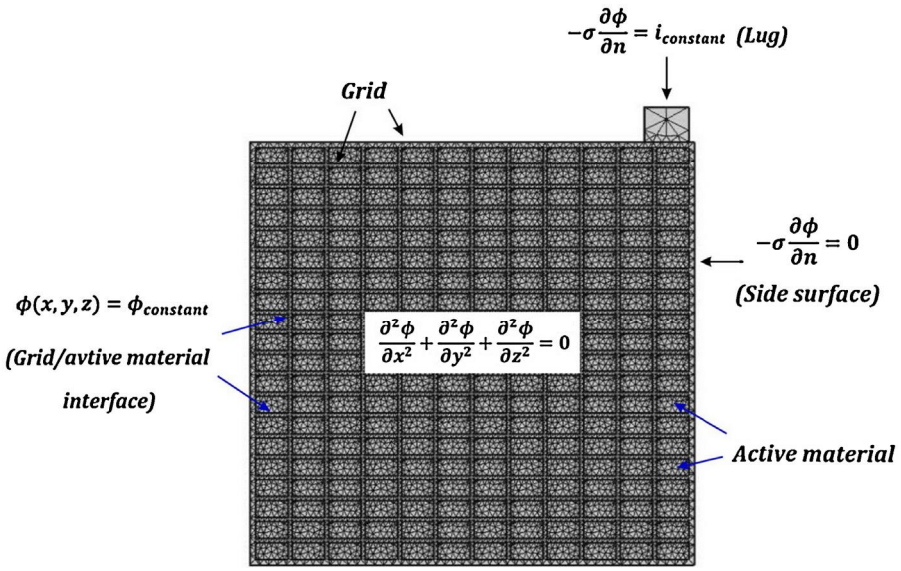

Fig. 2. A schematic of the domain used to study the conventional grid configuration. Boundary conditions are shown above.

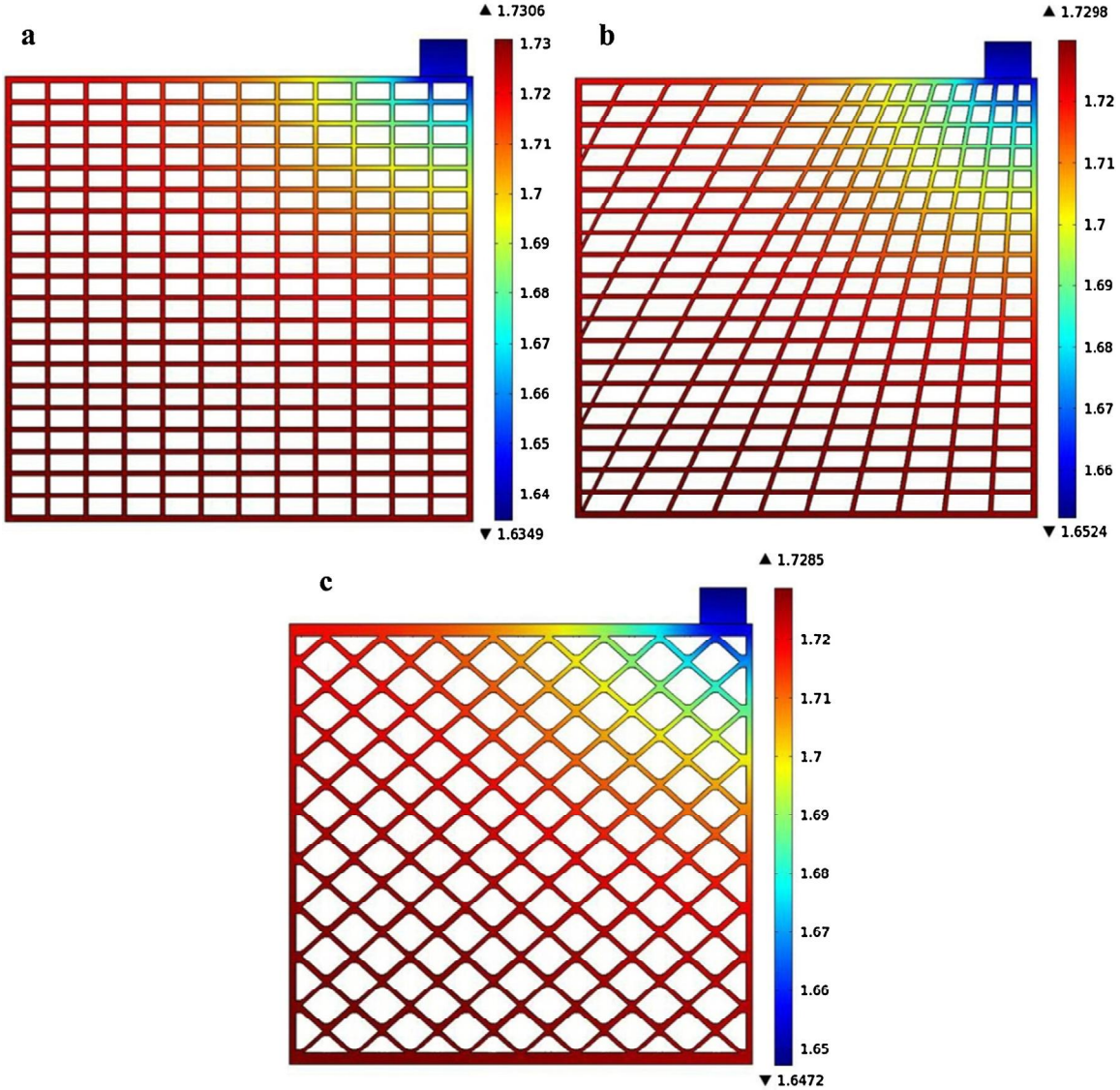

Fig. 3. Potential distributions (V) through grids with different configurations, i.e. (a) conventional, (b) diagonal and (c) expanded metal.

Table 2
Max. and min. potential values for conventional, diagonal and expanded metal grid configurations.

Grid name	E_{max} (V)	E_{min} (V)	Potential difference (mV)
Conventional	1.730	1.634	95.7
Diagonal	1.729	1.652	77.4
Expanded metal	1.728	1.647	81.3

As shown in Fig. 1b, wire density is much higher in upper right quarter of diagonal grid in compare to its other regions, whereas conventional grid consists of a uniform wire configuration (cf. Fig. 1a). Non-uniformity of wires results in lower ohmic resistance leading to better current flow toward the lug in diagonal grid. In other words, the current collecting ability of this grid is better than the other ones. The experimental data reported by Yamada et al. also confirmed that even partial radial grid configuration could effectively decrease the electric resistance and hence, reducing the potential drop at the grid for up to 25% [6].

The reticulated configuration of expanded metal grid introduces a skewed path for current toward the lug as well as higher wire density in regions near the frame edges in compare to central areas. Moreover, upper and lower horizontal edges of the grid frame are thicker than other parts improving the current collection ability of this particular grid configuration. As a result, ohmic resistance of the grid, particularly near the lug, is significantly reduced. Consequently, potential distribution in expanded metal grid is more uniform than the conventional grid.

Potential distributions through active material and adjacent electrolyte to the grid are demonstrated in Fig. 4. Since outer boundaries of electrolyte domain are set as insulators, their potential values assume to be zero (Fig. 4). As shown in Fig. 4, potential values gradually reach negative values from left lower corner of the grid to regions near the lug in all cases. Max and min potential values are tabulated in Table 3 for each case. Even though potential difference's value in case of diagonal grid configuration seems to be the lowest one, other cases reveal almost similar values with max margin of 18 mV.

Considering all grids possess same weight, the highest surface area of diagonal grid results in best contact surface between the active material and the grid wires. However, its non-uniform grid configuration results in uneven contact surface all over the grid.

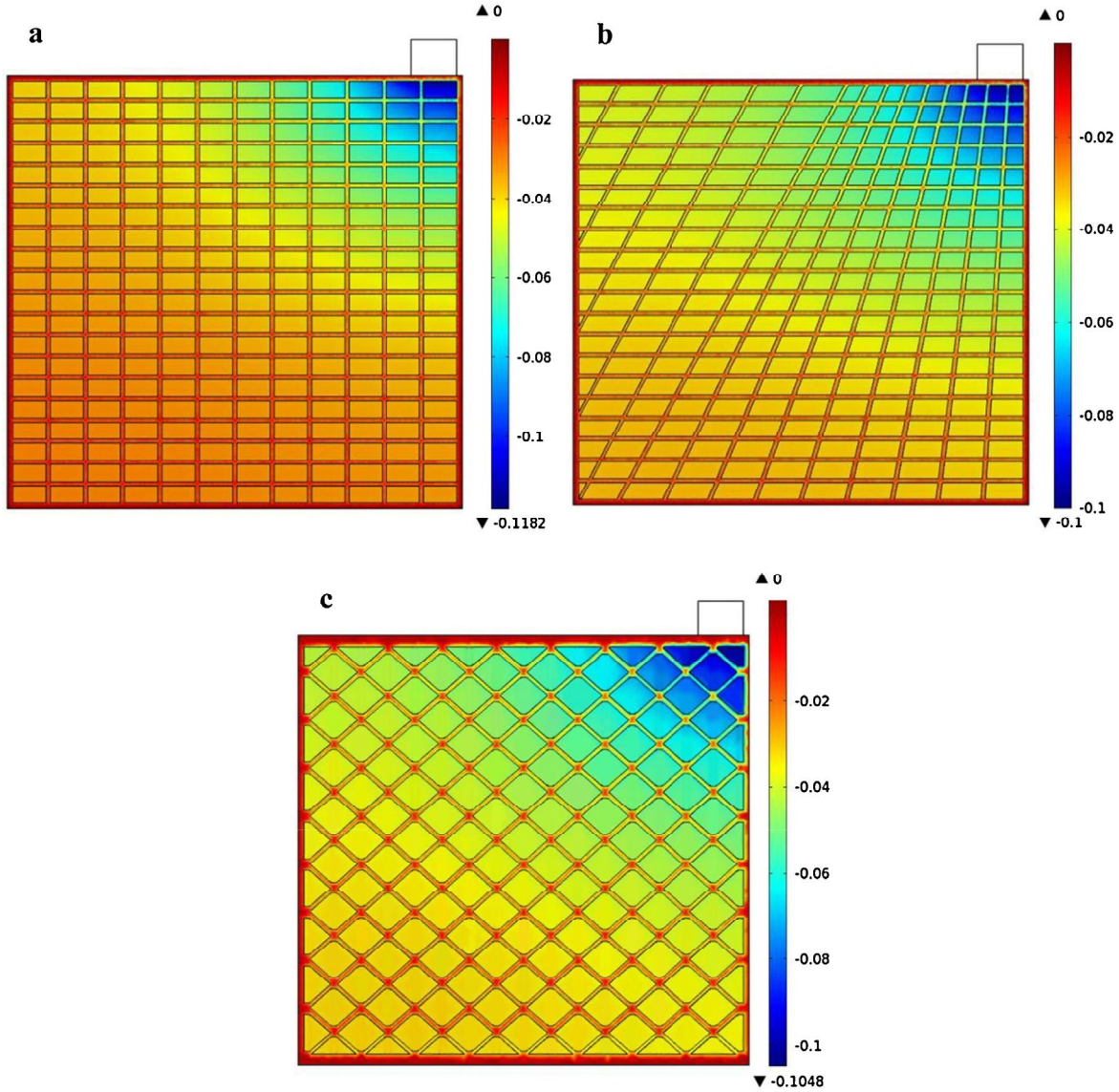

Fig. 4. Potential distribution (in V) through active material and adjacent electrolyte to the grid for (a) conventional grid, (b) diagonal grid, (c) expanded metal grid configurations.

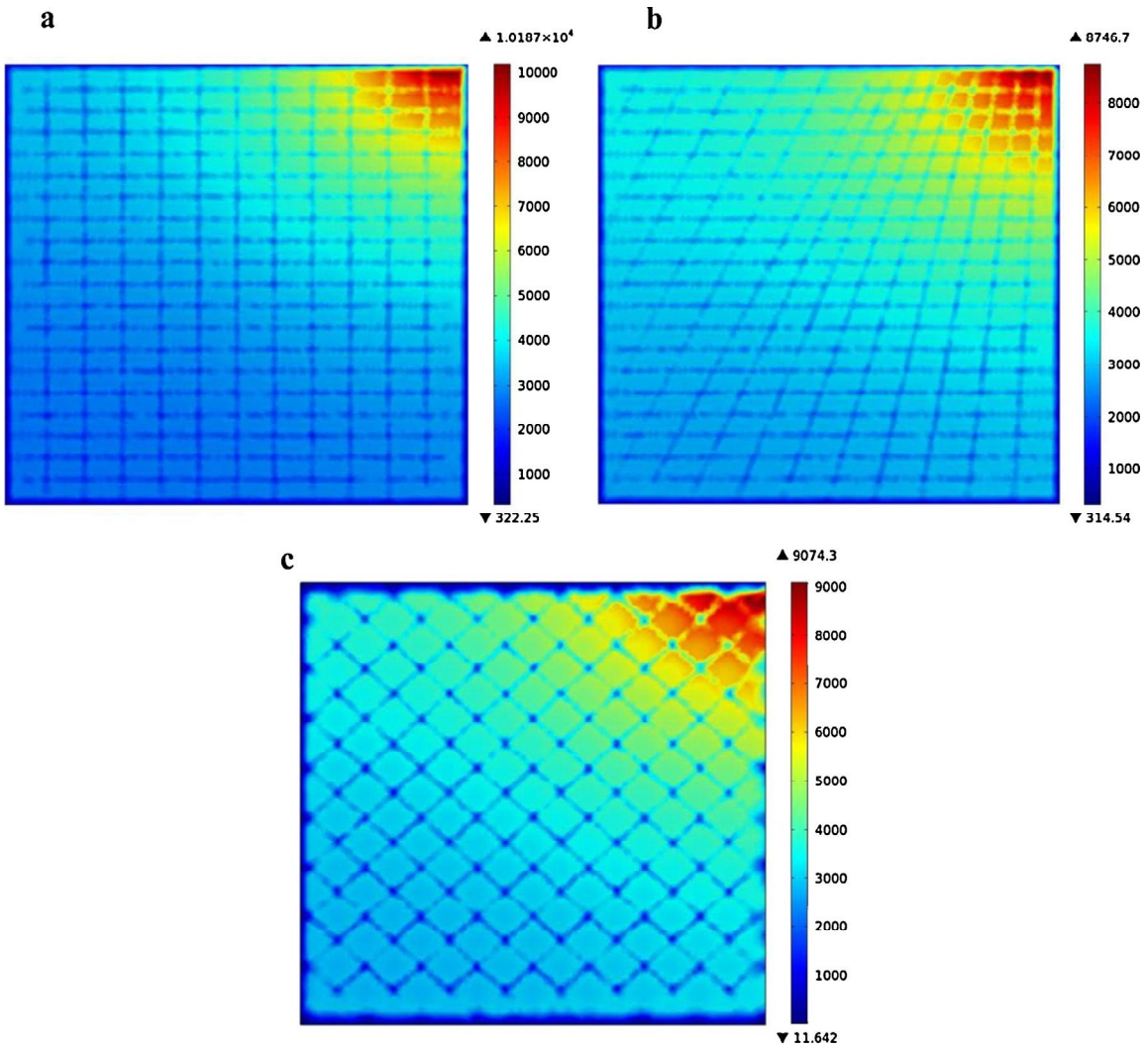

Fig. 5. Distributions of current density (A/m^2) in the electrolyte adjacent to surface of each grid with different configurations, i.e. (a) conventional grid, (b) diagonal grid and (c) expanded metal grid.

Table 3
Max. and min. potential values of active material and adjacent electrolyte to the grid in case of conventional grid, diagonal grid and expanded metal grid configurations.

Grid name	E_{max} (V)	E_{min} (V)	Potential difference (mV)
Conventional	0	-0.118	118
Diagonal	0	-0.100	100
Expanded metal	0	-0.104	104

Since the whole current produced in a battery plate passes through the lug, this section carries highest current density value. The effect of grid configuration on the distribution of current density in the electrolyte adjacent to surface of each plate has been shown in Fig. 5. Max and min values of current density in the electrolyte are tabulated in Table 4. It has been observed that the current density values decrease in all cases when we move from lug to lower left corner of the plate. This is mainly due to the ohmic resistance in the electrolyte. This is also supported by literature which Guo et al. reported uniform current density distribution for the most parts of the surface of the positive plate except near the log for conventional grid configuration at high discharge rate [14,15]. However, more uniform distribution of current density in the adjacent electrolyte is achieved by diagonal grid rather than conventional one. In the case of expanded metal grid, lowest current density in the adjacent electrolyte is observed.

Table 4
Max. and min. current density values in the electrolyte adjacent to surface of each grid configurations, i.e. conventional, diagonal and expanded metal grids.

Grid name	i_{max} (A/m^2)	i_{min} (A/m^2)
Conventional	10187	322
Diagonal	8746	314
Expanded metal	9076	11

4.2. Potential and current density distributions of Optimized diagonal grid

The increase in grid weight always follows by a decrease in potential drop over the grid. However, this raises production costs of a battery mainly because of higher amount of lead alloy used in each grid [6]. Hence, it is more favorable to reduce grid weight without affecting its current collecting ability. Optimization of the grid configuration is one solution to overcome potential drop due to ohmic resistance through the grid [16]. In 1996, Kao and Mrotek introduced a new design for the grid of lead–acid batteries with optimum current collection at the logs, maximizing performance of the battery while keeping its weight at a minimum [17].

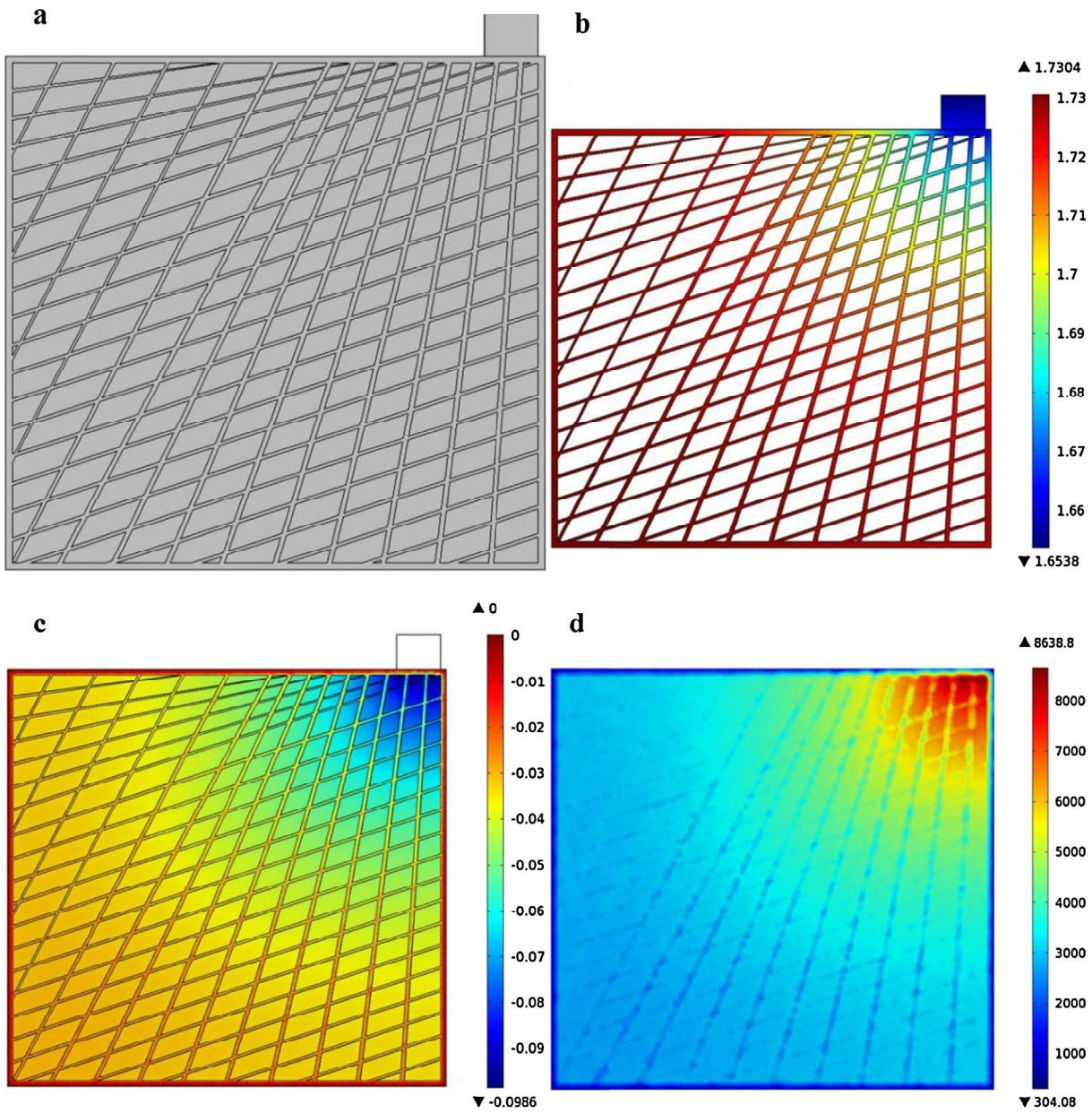

Fig. 6. Optimized diagonal grid: (a) a schematic of grid configuration, (b) potential distribution (V) in the grid and lug, (c) potential distribution (V) through active material and adjacent electrolyte to surface of the grid, (d) distribution of current density (A/m^2) in the electrolyte adjacent to surface of grid.

Fig. 6a shows a schematic of their proposed grid configuration which consists of a rectangular frame with two sets of skewed ribs. One set of grid wires tapers when moving from lug to the bottom of the grid. It should be mentioned that this grid is slightly optimized by adding another set of skewed ribs instead of horizontal ones from side to side. Since current conducting role of regions far from the lug is less significant than wires near it (cf. Figs. 3–5), any reduction in cross section of wires far from the lug may have negligible effect on potential and current distributions through the plate. As a result, weight of this optimized grid decreases to 105.2 g and weight of its associated active material increases to 254 g (cf. Table 1). Consequently, parameter α decreases to 0.292. Comparing to all other cases, optimized grid configuration achieves favorable low value of α with a margin of almost 19%. The maximum and minimum values of potential and current density of optimized diagonal plate are tabulated in Table 5. The potential difference of 77 mV in the optimized grid is close to the diagonal grid configuration. Same trend is also observed for the difference between max and min potential

Table 5
Max. and min. values of potential and current density of optimized diagonal plate.

Grid potentials		Active material and adjacent electrolyte to the grid potentials				Current density values of the electrolyte adjacent to surface	
E_{max} (V)	E_{min} (V)	Potential difference (mV)	E_{max} (V)	E_{min} (V)	Potential difference (mV)	i_{max} (A/m^2)	i_{min} (A/m^2)
1.730	1.653	77	0	−0.098	98	8638	304

values through active material and adjacent electrolyte to surface of the grid (see Table 5). It is interesting to know even though the grid weight is reduced and the designing parameters are improved, the differences in potential values are still the lowest ones among aforementioned grid configurations (cf. Table 2, Table 3, Table 5). Hence, the optimized grid configuration is more favorable. In another study by May et al., it is confirmed that the use of tapered wires in a positive plate of lead acid battery would result in much lower internal resistance as well as uniform use of both grid and active materials and hence, enhanced battery performance [16]. Clearly, more in-depth experimental studies on real-time performance of the grids in a battery coupled possibly with optimization of lug location as well as thickness of tapered/diagonal wires using numerical modelling techniques are required. However, these studies were beyond the objectives here as we emphasize on the use of numerical modelling methods as a fast and inexpensive method for optimization of the grid configuration.

5. Conclusion

The potential and current density distributions have been modeled via numerical methods to study the effect of grid configuration on the performance of a positive electrode in lead–acid batteries. An optimized grid design has been also studied via numerical modeling method to confirm its low grid weight as well as improved current collecting role. The following conclusions can be summarized according to the presented results:

1. Potential and current density distributions through a battery plate are significantly affected by different configurations of grids.
2. Higher density of grid wires in regions near the lug results in uniform distributions of potential and current density all over the plate.
3. In compare to conventional grid configuration, which consists of a set of parallel horizontal and vertical ribs surrounded by a rectangular frame, diagonal configuration of grid wires results in more uniform potential distribution all over the plate, mainly due to its skewed wires.
4. Regions far from lug exhibit the lowest variations of potential and current density. Hence, a reduction in the cross sectional area of skewed ribs in these areas not only has negligible effect on potential and current density distributions but also can reduce total weight of the plate.

Numerical modeling is a fast and inexpensive method for optimization of the grid configuration. Different configurations of battery grid can be fully investigated using this method to find the optimum configuration with the most uniform potential and current density distributions regardless of difficulties associated with experimental studies. Our future work will aim at more extensive investigations on the real-time performance of the grids in lead–acid batteries together with the optimization of lug location as well as thickness of tapered/diagonal wires using numerical modelling techniques.

References

[1] R.D. Prengaman, Journal of Power Sources 95 (2001) 224–233.
[2] S. Fouache, A. Chabrol, G. Fossati, M. Bassini, M.J. Sainz, L. Atkins, Journal of Power Sources 78 (1999) 12–22.
[3] J.E. Manders, N. Bui, D.W.H. Lambert, J. Navarette, R.F. Nelson, E.M. Valeriote, Journal of Power Sources 73 (1998) 152–161.
[4] R. Ponraj, S.D. McAllister, I.F. Cheng, D.B. Edwards, Journal of Power Sources 189 (2009) 1199–1203.
[5] P. Hosseini Benhangi, D. Nakhaie, M.H. Moayed, A. Molazemi, Journal of Power Sources 196 (2011) 10424–10429.
[6] K. Yamada, K.-i. Maeda, K. Sasaki, T. Hirasawa, Journal of Power Sources 144 (2005) 352–357.
[7] D. Pavlov, Lead–Acid Batteries: Science and Technology, Elsevier Science, Amsterdam, 2011.
[8] R.J. Ball, R. Evans, R. Stevens, Journal of Power Sources 103 (2002) 213–222.
[9] M. Calábek, K. Micka, P. Bača, P. Křivák, Journal of Power Sources 85 (2000) 145–148.
[10] E. Kroutilova, I. Behunek, P. Fiala, in: S. Wiak, A. Krawczyk, I. Dolezel (Eds.), Numerical Model of Optimization Lead–Acid Accumulator Grids Intelligent Computer Techniques in Applied Electromagnetics, 119, Springer Berlin/Heidelberg, 2008, pp. 223–230.
[11] D. Pavlov, Journal of Power Sources 53 (1995) 9–21.
[12] K.R. Bullock, Journal of Power Sources 51 (1994) 1–17.
[13] K. McGregor, Journal of Power Sources 59 (1996) 31–43.
[14] Y. Guo, Y. Li, G. Zhang, H. Zhang, J. Garche, Journal of Power Sources 124 (2003) 271–277.
[15] Y. Guo, H. Liu, Journal of Power Sources 183 (2008) 381–387.
[16] G.J. May, N. Maleschitz, H. Diermaier, T. Haeupl, Journal of Power Sources 195 (2010) 4520–4524.
[17] E.N. Mrotek, W.-H. Kao, in: U.S. Patent (Ed.), Lead–Acid Batteries with Optimum Current Collection at Grid Lugs, Globe-Union, Inc., USA, 1996.